Asian Journal of Chemistry; Vol. 38, No. 8 (2026), 2191-2198
ASIAN JOURNAL OF CHEMISTRY
https://doi.org/10.14233/ajchem.2026.36474

Isolation, Structural Characterisation and Antifertility Assessment of a Novel Flavonol Glycoside from *Rivea hypocrateriformis*

S.S. GODIPURGE[1], M.T. PADMAJA[2], S. CHANDRASEKHAR[3], S. YALLAPPA[4,*], BASAVARAJ S. HUNGUND[5], ANUSHA MARALAGALA NAGARAJU[6] and P.H. SUNITHA[7]

[1]Departmetn of P.G. Studies and Research in Chemistry, Gulbarga University, Kalaburagi-585106, India
[2]Department of Chemistry, Vijaya College, R.V. Road, Basavanagudi, Bengaluru-560011, India
[3]Department of Physics, BNM Institute of Technology, Bengaluru-560070, India
[4]Department of Chemistry, Cambridge Institute of Technology, Bengaluru-560036, India
[5]Bioresource Development Laboratory, Department of Biotechnology, KLE Technological University, Hubballi-580031, India
[6]Department of Electronics and Communication Engineering, BGS Institute of Technology, (Affiliated to Adichunchanagiri University), B G Nagara-571811, India
[7]Department of Electronics and Communication Engineering, M.S. Engineering College, Bengaluru-562110, India

*Corresponding author: E-mail: yallappashiralgi5@gmail.com

Received: 21 May 2026 *Accepted*: 26 July 2026 *Published online*: 7 August 2026 AJC-22447

The aim of this study was to identify and characterise a novel flavonoid glycoside, hypocroside (compound **1**), isolated from *Rivea hypocrateriformis* and evaluate its antifertility activity. The ethanolic extract of the aerial parts of *R. hypocrateriformis* was fractionated by chromatographic techniques, and the structure of the novel compound was elucidated using ^{1}H NMR, ^{13}C NMR, mass spectrometry, TLC and HPLC analyses. The ethyl acetate fraction (FERH) and the isolated compound (compound **1**) were selected from the crude extract for biological evaluation. Their antifertility activity was assessed in rats using anti-implantation, estrogenic and anti-estrogenic assays. FERH and compound **1** exhibited anti-implantation activity at doses of 100 and 200 mg/kg body weight and 12.50 and 25 mg/kg body weight, respectively. Both treatments exhibited significant anti-estrogenic activity and increased uterine weight in immature ovariectomised rats. The reduction in the number of implantation sites in female rats confirmed the antifertility activity of compound **1** and identified it as a promising antifertility agent with anti-estrogenic potential. Molecular docking analysis examined the binding of compound **1** with the target protein. Compound **1** formed hydrogen bonds with PHE337 (2.63 Å), GLN414 (2.57 and 2.38 Å), ASN407 (2.39 Å), SER341 (2.34 Å) and ASP411 (2.68 Å). The molecular docking results and the *in vitro* anti-estrogenic activity support the role of compound **1** as an inhibitor of the estrogen receptor.

Keywords: *Rivea hypocrateriformis*, Flavonoid glycoside, Hypocroside, Antifertility activity.

INTRODUCTION

Herbal remedies have been used in traditional medicine for centuries and remain an important source of bioactive compounds for the prevention and treatment of a wide range of human diseases [1,2]. Medicinal plants are rich in structurally diverse secondary metabolites with significant pharmacological properties, making them valuable resources for the discovery of novel therapeutic agents [3]. Among these, plant derived antifertility compounds have received considerable attention as potential alternatives to synthetic contraceptives because of their therapeutic potential and natural origin [4,5]. Several medicinal plants possess antifertility activity, which has been associated with the presence of phytoestrogens and other bioactive constituents capable of modulating reproductive function [4]. Flavonoids, particularly flavonol glycosides, constitute an important class of phytochemicals with estrogenic and anti-estrogenic activities relevant to antifertility research [4]. These properties make flavonol glycosides attractive candidates for the development of plant-based antifertility agents.

Rivea hypocrateriformis is a vigorous woody climbing shrub in the Convolvulaceae family that grows in subtropical forests of India and Pakistan. The indigenous people of Karnataka state of India use the plant medicinally to treat a

variety of illnesses, including malaria and to reduce pain. The plant has been reported to possess anticancer, antidiabetic, anti-inflammatory, antidepressant and analgesic activities, and has traditionally been used for the treatment of burns, piles and pregnancy interruption [6,7]. Phytochemical investigations have revealed that *R. hypocrateriformis* contains alkaloids, glycosides, tannins, saponins, phenolic compounds, steroids and flavonoids [5]. Zamarrud *et al.* [8] reported the isolation of desmethyl bergenin hemihydrate from *R. hypocrateriformis*. The chemical diversity of this species makes it a valuable source of bioactive metabolites with therapeutic relevance. Preliminary screening of the ethanolic extract of the aerial parts of *R. hypocrateriformis* exhibited anti-implantation activity, justifying further phytochemical investigation. This study describes the isolation and structural characterisation of a novel flavonoid glycoside, hypocroside (compound **1**), from the aerial parts of *R. hypocrateriformis*. The antifertility activity of the isolated compound was evaluated through anti-implantation, estrogenic and anti-estrogenic assays and its interaction with the estrogen receptor was examined by molecular docking.

EXPERIMENTAL

In this experiment, all chemicals and reagents were of analytical grade and used as such. Thin-layer chromatography (TLC) and column chromatography were performed using silica gel 60 F_{254} plates and silica gel (60-120 mesh) (Merck), respectively. Analytical HPLC was performed on an Agilent 1200 Series system equipped with a multi-wavelength UV/VIS detector (254 nm) using a Zorbax RX-C18 column (150 × 4.6 mm, 5 μm; Agilent Technologies). UV-Vis spectra were recorded on a UV-Vis spectrophotometer, FTIR spectra on a Nicolet Impact 400 FTIR spectrophotometer using KBr pellets and ^{1}H & ^{13}C NMR spectra on a Bruker 600 MHz spectrometer in $CDCl_3$ with TMS as the internal standard. Melting points were determined in open capillaries and are uncorrected.

The aerial parts of *R. hypocrateriformis* were collected from Belur, Bidar district, India. The plant was authenticated by the Department of Botany, Gulbarga University and a voucher specimen (HGUG No. 90) was deposited in the departmental herbarium for future reference.

Extraction: The aerial parts of *R. hypocrateriformis* (2.5 kg) were air-dried and crushed prior to 48 h Soxhlet extraction. The ethanol extract was concentrated under reduced pressure in a rotary evaporator to yield 150 g of crude ethanol extract, which was suspended in water. Petroleum ether and ethyl acetate were used to extract the solution further. After extracting the solvent, the ethyl acetate extract (25 g) was partitioned using silica gel column chromatography and eluted with a $CHCl_3$-MeOH gradient (95:5% MeOH) to yield six fractions. To obtain compound **3**, fraction 1 was treated to column chromatography (silica gel, $CHCl_3$-MeOH, 10:1) (10 mg). Fractions 2 to 4 were purified further using RP-18 column chromatography and eluted with MeOH-H_2O (20% and 40% MeOH) to yield compound **2**. (18 mg). From fractions 5 and 6, compound **1** was purified using column chromatography with silica gel and the solvent system $CHCl_3$-MeOH (2:1). Then, the isolated compound **1** (93 mg) was further purified by RP-18 column chromatography.

Experimental animals: *An albino* male adult Wistar rats (180-220 g) of either sex were obtained from the Central Animal House of the M.R. Medical College, Gulbarga, India. Rats were randomly divided into five groups (n = 6) and maintained under standard laboratory conditions (20 ± 2 ºC, 50% relative humidity and a 12 h light/12 h dark cycle). Animals received a commercial pellet diet (Amrut Laboratories, Pranava Agro Industries Ltd., Sangli, India) and water *ad libitum*. All experimental procedures were approved by the Institutional Animal Ethics Committee (No. HKES COP/IAEC/2012/54) and conducted in accordance with CPCSEA guidelines [9].

Acute toxicity studies: Wistar albino rats weighing 180-220 g of either sex were used. The study was conducted in accordance with OECD guidelines [9] and no adverse effects or mortality were observed in mice and rats given up to 4000 mg/kg over a 24 h period. The animals were monitored daily for mortality and moribund status.

Anti-implantation (antifertility) activity: The anti-implantation study was conducted in accordance with the recommendations by Ferreira *et al.* [10]. The vaginal smear of each female rat was examined daily and only rats in their normal estrous cycle were selected. At the beginning of the estrous cycle, female rats in the proestrous phase were confined overnight with male rats of proven fertility in a 2:1 ratio and the next morning, vaginal smears from each rat were examined for indications of copulation. The next day was designated as the beginning of pregnancy. The pregnant female rats were randomly divided into six groups, each consisting of six animals. Group I received 1% Tween 80 and served as the vehicle control. Group II received tamoxifen (10 mg/kg body weight) as the positive control. Groups III and IV received the ethyl acetate fraction (FERH) of *R. hypocrateriformis* at doses of 100 and 200 mg/kg body weight, respectively. Groups V and VI received the isolated flavonol glycoside, compound **1**, at doses of 12.5 and 25 mg/kg body weight, respectively. Beginning on day 1, the phytocompounds were delivered orally *via* catheter tube for 7 consecutive days. All of the animals were laparotomised on the 10th day of pregnancy under light ether anaesthesia. The number of implants implanted in both uterine horns was counted. The anti-implantation percentage was calculated by using formula:

$$\text{Anti-implantation (\%)} = \frac{I_c - I_t}{I_c} \times 100$$

where I_c = number of implantation sites in control; and I_t = number of implantation sites in test.

Anti-estrogenic activity: Under light ether anesthesia and aseptic conditions, immature female albino rats (21-23 days old; weighing 35-45 g) were bilaterally ovariectomised using the dorsolateral approach as previously described [11]. After recovery, the animals were randomly divided into six groups, with six rats in each group. Group I received 1% Tween 80 and served as the vehicle control. Group II received tamoxifen (10 mg/kg body weight) as the positive control. Groups III and IV received the ethyl acetate fraction (FERH) of *R. hypocrateriformis* at doses of 100 and 200 mg/kg body weight, respectively. Groups V and VI received the isolated

flavonol glycoside, compound **1**, at doses of 12.5 and 25 mg/kg body weight, respectively.

All treatments were administered orally once daily for 7 consecutive days. On the 8th day, the animals were anesthetised with light ether and sacrificed. The final body weight, vaginal opening and vaginal cornification were recorded before sacrifice. The uterus was carefully excised, blotted free of surrounding tissues and weighed immediately using an analytical balance. Blood samples were collected and serum was separated for biochemical analysis, including the estimation of estrogen and cholesterol levels.

Molecular docking simulation: The X-ray crystal structure of the human estrogen receptor ligand-binding domain complexed with 17β-estradiol (PDB ID: 1ERE) was retrieved from the RCSB Protein Data Bank. The structure of hypocroside (compound **1**) was drawn in two dimensions and energy-minimised in three dimensions using ACD/ChemSketch. Protein and ligand structures were prepared for molecular docking using AutoDock Tools 1.5.6 following the reported protocol [12]. The binding site was selected according to an earlier study [13]. A grid box of 40 × 40 × 40 Å was generated with grid center coordinates of x = 9.529568, y = 45.998682 and z = 131.374773.

Molecular docking was performed using AutoDock Vina 1.1.2. Flexible ligand docking was carried out by treating the receptor as rigid while allowing the ligand ten rotatable bonds. Docking poses were ranked according to binding affinity, and the top-ranked pose with the lowest RMSD was selected for interaction analysis. Protein–ligand interactions were visualised using BIOVIA Discovery Studio Visualizer 2021. Binding affinity, hydrogen bonds, hydrophobic interactions and other non-bonded contacts were used to evaluate the binding interactions between compound **1** and the estrogen receptor [14].

Molecular dynamics simulation: Molecular dynamics (MD) simulations were performed using GROMACS 2018.1. The docked human estrogen receptor-compound **1** complex with the highest binding affinity was selected for simulation following the protocol described by Patil *et al.* [15]. The protein-ligand complex, comprising 3,860 residues with 3,795 protein backbone atoms, was simulated for 100 ns under NPT conditions at 310 K and 1 bar pressure. Trajectory analyses, including root-mean-square deviation (RMSD), root-mean square fluctuation (RMSF), radius of gyration (Rg), ligand-protein hydrogen bonds and solvent-accessible surface area (SASA), were performed using QtGrace [15].

Statistical analysis: The data were presented as mean ± SEM and statistical significance was determined using one-way ANOVA followed by Student's *t*-test. $p < 0.05$ and $p < 0.001$ were considered significant values.

RESULTS AND DISCUSSION

Hypocroside (compound **1**) is obtained as pale-yellow gummy (93 mg) from the aerial parts of *R. hypocrateriformis* as shown in Fig. 1. The FTIR spectrum of compound **1** exhibited a broad absorption band at 3446 cm^{-1}, which is the characteristic of hydroxyl (–OH) groups. Absorption bands at 2964, 2920, 2854 and 2445 cm^{-1} were assigned to the symmetric and asymmetric C–H stretching vibrations of

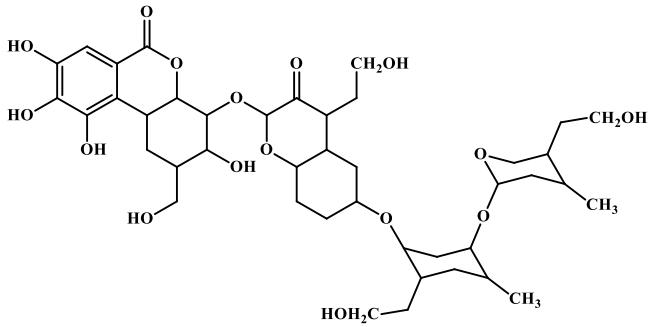

Fig. 1. Structures of hypocroside isolated from ethanolic extract of *R. hypocrateriformis*

methyl and methylene groups. The bands at 1744 and 1735 cm^{-1} were assigned to the carbonyl stretching vibrations of the lactone and α,β-unsaturated carbonyl groups, respectively, while the absorption band at 1264 cm^{-1} was attributed to C–O–C stretching.

The ^{1}H NMR spectrum of compound **1** was also consistent with the proposed structure and showed signals at δ 0.86 (s, 6H, 2 × CH_3), δ 1.50 (m, 17H, 17 × CH), δ 1.30-3.60 (m, 30H, 15 × CH_2), δ 4.25 (t, 5H, 5 × OH), δ 5.70 (t, 3H, 3 × CH) and δ 7.20 (m, 1H, Ar–H). The ^{13}C NMR spectrum accounted for all 42 carbon atoms of the molecule. Signals at δ 13.81 were assigned to two methyl carbons, whereas resonances at δ 22.18 and 38.91 corresponded to methylene carbons of the CH_2-CH_2-OH moiety. Aromatic carbon resonances appeared between δ 143.13 and 168.53, while signals at δ 29.93 and 59.83 were assigned to the CH_2-CH_2-OH side chain. The carbonyl carbons resonated at δ 206.93, and signals at δ 31.32, 48.18, 29.93 and 59.83 were attributed to the alicyclic ring carbons.

The mass spectrum showed a molecular ion peak at *m/z* 823 ($[M+H]^+$), consistent with the molecular weight of compound **1**. The fragmentation pattern (Fig. 2) generated prominent ions at *m/z* 796 (11%), 317 (90%) and 348 (100%). The ion at *m/z* 317 resulted from the loss of a $C_{11}H_{20}O_4$ fragment, whereas the base peak at *m/z* 348 underwent further fragmentation through the loss of CO_2 and a CHO radical to yield a fragment ion at *m/z* 276 (98%). This fragmentation pattern supports the proposed structure of the compound **1**.

HPLC analysis of compound **1** was performed at 254 nm. The chromatogram contained peaks at retention times of 3.356, 4.014, 8.717 and 9.251 min, with the peak at 3.356 min representing the major constituent of the extract. Flavonoid peaks were identified by comparing their retention times (3.108, 3.303, 3.521 and 4.063 min) with that of the quercetin standard. Peak identities were confirmed by co-injection of the corresponding standard, which resulted in an increase in peak intensity without any change in retention time. Quercetin eluted at a retention time of 3.108 min and was well resolved from the remaining peaks. The chromatographic profile confirmed the isolation and purity of compound **1**. The same procedure was followed for all reference standards. Thus, based on the combined chromatographic and spectroscopic analyses, compound **1** was identified as 3,8,9,10-tetrahydroxy-4-((4-(2-hydroxyethyl)-6-(((2*R*,5*R*)-2-(2-hydroxy-ethyl)-5-(((2S, 4R,5S)-5-(2-hydroxyethyl)-4-methyltetrahydro-2*H*-pyran-2-

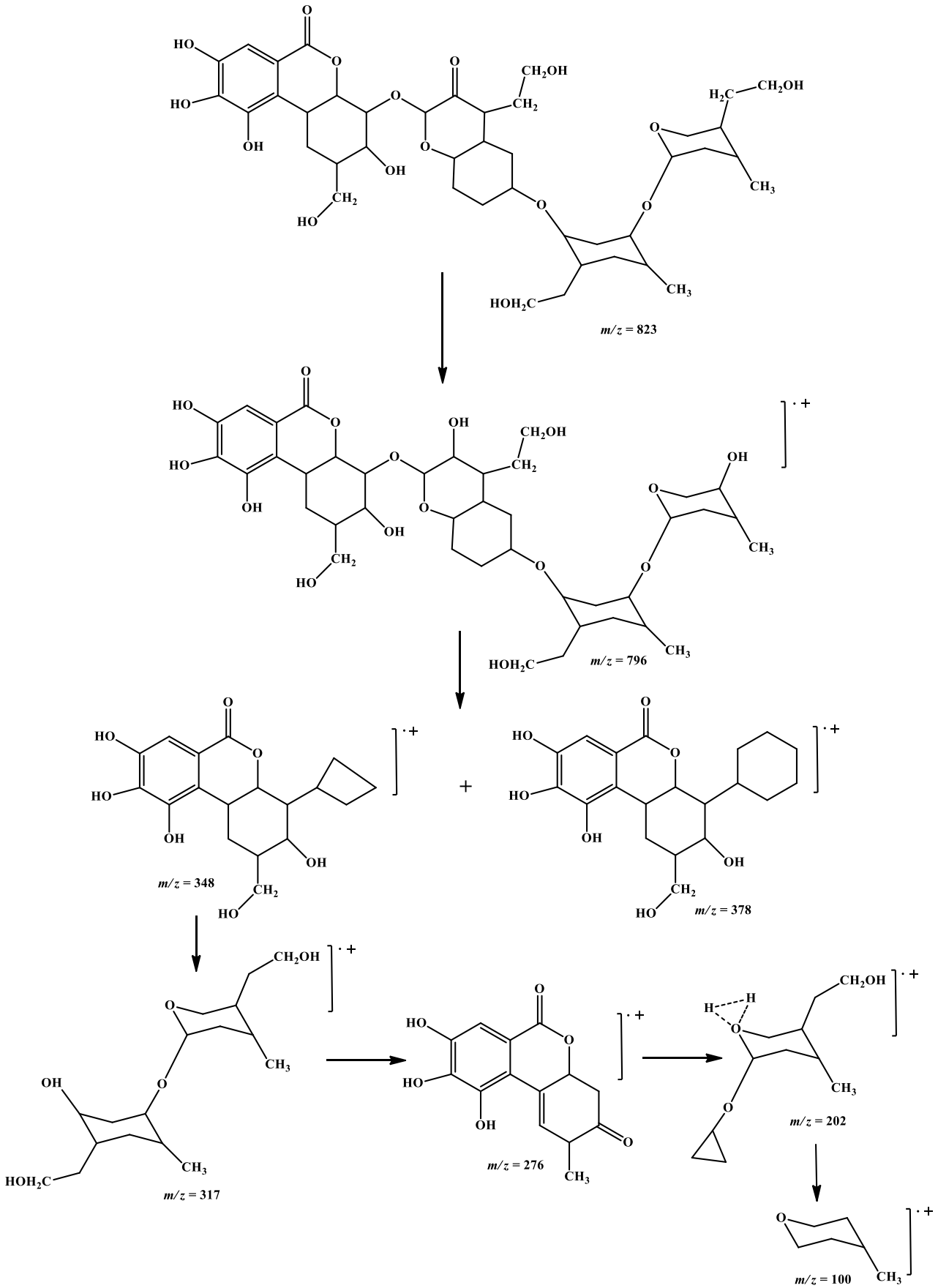

Fig. 2. Mass fragmentation of compound **1** (hypocroside)

yl)oxy)-4-methylcyclohexyl)oxy)-3-oxooctahydro-2H-chromen-2-yl)oxy)-2-(hydroxymethyl)-2,3,4,4a-tetrahydro-1*H*-benzo[*c*]chromen-6(10*bH*)-one.

Acute toxicity and anti-implantation activity: Acute oral toxicity studies demonstrated that the ethyl acetate fraction (FERH) and compound **1** were well tolerated in Wistar albino rats at doses up to 4000 mg/kg body weight, with no mortality or observable signs of toxicity during the experimental period. These findings support a favourable safety profile under the tested conditions. The anti-implantation activity of the positive control (tamoxifen), FERH and compound **1** is shown in Table-1. Tamoxifen, used as the positive control, exhibited the highest anti-implantation activity (77.55%), validating the experimental model. FERH exhibited dose-dependent anti-implantation activity, with inhibition increasing from 35.53% at 100 mg/kg to 63.36% at 200 mg/kg. Compound **1** exhibited even higher anti-implantation activity, increasing from 68.25% at 12.5 mg/kg to 75.55% at 25 mg/kg. The higher inhibitory activity of compound **1** is relative to the ethyl acetate fraction, which identifies this compound as a major contributor to the antifertility activity of *R. hypocrateriformis*.

Compound **1** exhibited anti-implantation activity comparable to that of tamoxifen while maintaining a favourable safety profile, making it a promising natural antifertility candidate. Both FERH and Compound **1** exhibited a clear dose-dependent increase in anti-implantation activity, emphasising the biological relevance of the isolated compound. The observed antifertility effect is likely associated with modulation of the hormonal milieu essential for implantation. Disruption of the estrogen-progesterone balance during early pregnancy can reduce uterine receptivity and interfere with embryo implantation, leading to a lower implantation rate. Comparable mechanisms have been reported for several plant-derived flavonoids with antifertility properties [16].

Anti-estrogenic activity: The anti-estrogenic activity of the positive control (tamoxifen), FERH and compound **1** is shown in Table-2, while the corresponding serum estrogen and cholesterol levels are presented in Fig. 3. Tamoxifen exhibited the highest uterine weight among all treatment groups, confirming the responsiveness of the experimental model. This response agrees with its well-established role as a selective estrogen receptor modulator (SERM), which exerts partial estrogenic effects in uterine tissue while antagonising estrogen receptor signalling in other target organs [17].

Administration of FERH and compound **1** significantly altered uterine weight relative to the vehicle control. FERH caused a moderate increase in uterine weight, whereas hypocroside at 12.5 mg/kg elicited the highest uterotrophic response among the test compounds. Uterine weight at 25 mg/kg was lower than that observed at 12.5 mg/kg despite the higher dose, which may reflect a non-linear response involving differential regulation of estrogen receptor signalling. Treatment with FERH and compound **1** was accompanied by changes in serum estrogen and cholesterol concentrations (Fig. 3). FERH at 100 mg/kg and compound **1** at 25 mg/kg were associated with higher serum estrogen levels than the control group, whereas FERH at 200 mg/kg and compound **1** at 12.5 mg/kg exhibited comparatively lower estrogen concentrations. Cholesterol concentrations differed across the treatment groups in a dose-related manner. Given its central role as the precursor for steroid hormone biosynthesis, alterations in cholesterol metabolism can influence estrogen and progesterone production and consequently, reproductive hormone homeostasis [18,19].

TABLE-1
ANTI-IMPLANTATION ACTIVITY OF POSITIVE CONTROL (TAMOXIFEN), ETHYL ACETATE FRACTION (FERH) AND HYPOCROSIDE (COMPOUND **1**)

Test compounds	Dose (mg/kg body weight)	Body weight gain (g) (Mean ± SEM)	% Inhibition of implantation sites (Mean ± SEM)	Anti-implantation (%)
Control (1% Tween 80)	–	46.155 ± 0.72	8.68 ± 0.26	–
Tamoxifen (positive control)	10	50.32 ± 0.25	1.95 ± 0.32**	77.55
FERH	100	32.94 ± 1.47	5.60 ± 0.59*	35.53
FERH	200	42.92 ± 1.29	3.18 ± 0.47**	63.36
Hypocroside (compound **1**)	12.50	41.38 ± 0.47	2.76 ± 0.46**	68.25
Hypocroside (compound **1**)	25.00	37.94 ± 0.57	2.12 ± 0.47**	75.55

Values are expressed as mean ± SEM (n = 6). Statistical significance was analysed using one-way ANOVA followed by Student's *t*-test. $p < 0.05$ and $p < 0.001$ compared with the vehicle control group.

TABLE-2
ANTI-ESTROGENIC ACTIVITY OF POSITIVE CONTROL (TAMOXIFEN), ETHYL ACETATE FRACTION (FERH) AND HYPOCROSIDE (COMPOUND **1**)

Test compounds	Dose (mg/kg)	Initial body weight (g)	Final body weight (g)	Body weight gain (g)	Uterine weight (mg)
Control (1% Tween 80)	–	35.40 ± 1.76	40.90 ± 1.73	5.50 ± 3.08	34.00 ± 0.91
Tamoxifen (positive control)	10	44.52 ± 0.92	59.64 ± 0.82	15.12 ± 0.50	69.49 ± 1.23**
FERH	100	25.19 ± 1.55	73.13 ± 0.87	47.90 ± 1.77	38.72 ± 1.44**
FERH	200	36.37 ± 1.61	39.30 ± 1.74	2.93 ± 1.98	42.80 ± 1.99*
Hypocroside (compound **1**)	12.50	41.90 ± 1.78	50.64 ± 1.81	8.71 ± 2.33	64.39 ± 1.33
Hypocroside (compound **1**)	25.00	37.20 ± 0.78	53.59 ± 0.56	16.48 ± 0.90	39.40 ± 1.74*

Values are expressed as mean ± SEM (n = 6). Statistical significance was analysed using one-way ANOVA followed by Student's *t*-test. $p < 0.05$ and $p < 0.001$ compared with the vehicle control group.

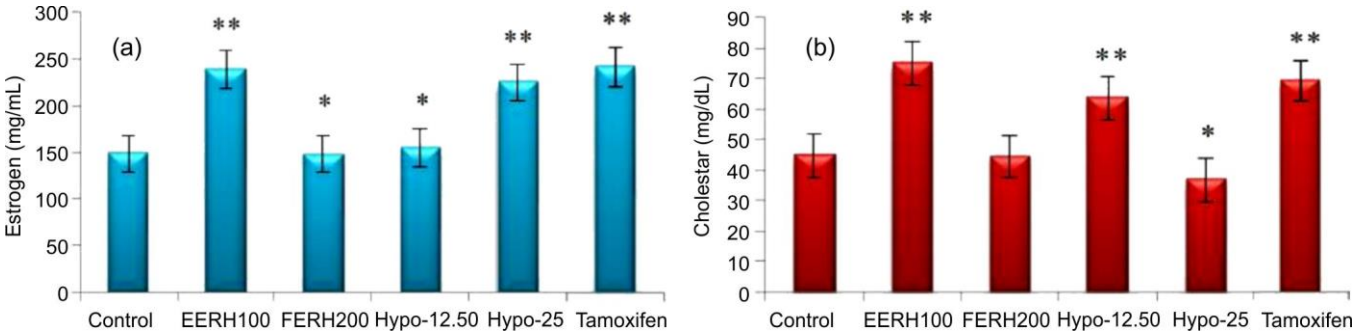

Fig. 3. Effect of the positive control (tamoxifen), ethyl acetate fraction (FERH), and hypocroside (compound **1**) on serum estrogen (a) and cholesterol (b) levels in ovariectomized immature female rats

Molecular docking simulation: Compound **1** formed hydrogen bonds with the residues PHE 337 (2.63 Å), GLN 414 (2.57 Å), GLN 414 (2.38 Å), ASN 407 (2.39 Å), SER 341 (2.34 Å) and ASP 411 (2.68 Å). It also formed an electrostatic pi-anion bond with ASP 411 (4.60 Å) and a hydrophobic alkyl bond with LEU 345 (4.19 Å). With these interactions, compound **1** showed a binding affinity of -8.2 kcal/mol and a similar binding pattern was obtained from previous study [20]. With the *in vitro* results depicting its anti-estrogenic activity, it can be concluded that compound **1** could act as a potential estrogen-receptor inhibitor. The visualisation of binding interactions of HYPO with the target protein has been given in Fig. 4. The molecular docking analysis demonstrated a favourable interaction between compound **1** and the human estrogen receptor, supporting the potential molecular basis of its observed antifertility activity. However, the docking results should be interpreted as supportive computational evidence rather than a direct measure of biological potency. Although comparative docking with established estrogen receptor ligands such as estradiol and tamoxifen was not performed in the present study, the observed binding affinity and key protein-ligand interactions suggest that compound **1** can effectively interact with the receptor binding pocket.

Molecular dynamics simulation: Molecular dynamics (MD) simulations were performed to evaluate the stability of the protein-compound **1** complex over a 100 ns simulation period. Structural stability was assessed using root-mean-square deviation (RMSD), root-mean-square fluctuation (RMSF), radius of gyration (Rg), solvent-accessible surface area (SASA), ligand RMSD and protein-ligand hydrogen bond analyses. RMSD was used to monitor conformational stability throughout the simulation, whereas RMSF provided information on residue-wise flexibility. The radius of gyration (Rg) was used to assess the compactness of the protein structure, and SASA was analysed to examine changes in solvent exposure.

The RMSD profiles of the protein backbone and the protein-compound **1** complex reached equilibrium within the range of 0.25-0.30 nm, with only minor fluctuations during the remainder of the simulation (Fig. 5). RMSF analysis identified relatively higher fluctuations in the N-terminal, C-terminal and loop regions, whereas the remaining residues exhibited limited mobility. The Rg values remained stable at approximately 2.35 nm and the protein retained its structural compactness throughout the simulation. SASA values exhibited only minor fluctuations, with the protein backbone ranging from 200 to 210 nm^2 and the protein–compound **1** complex

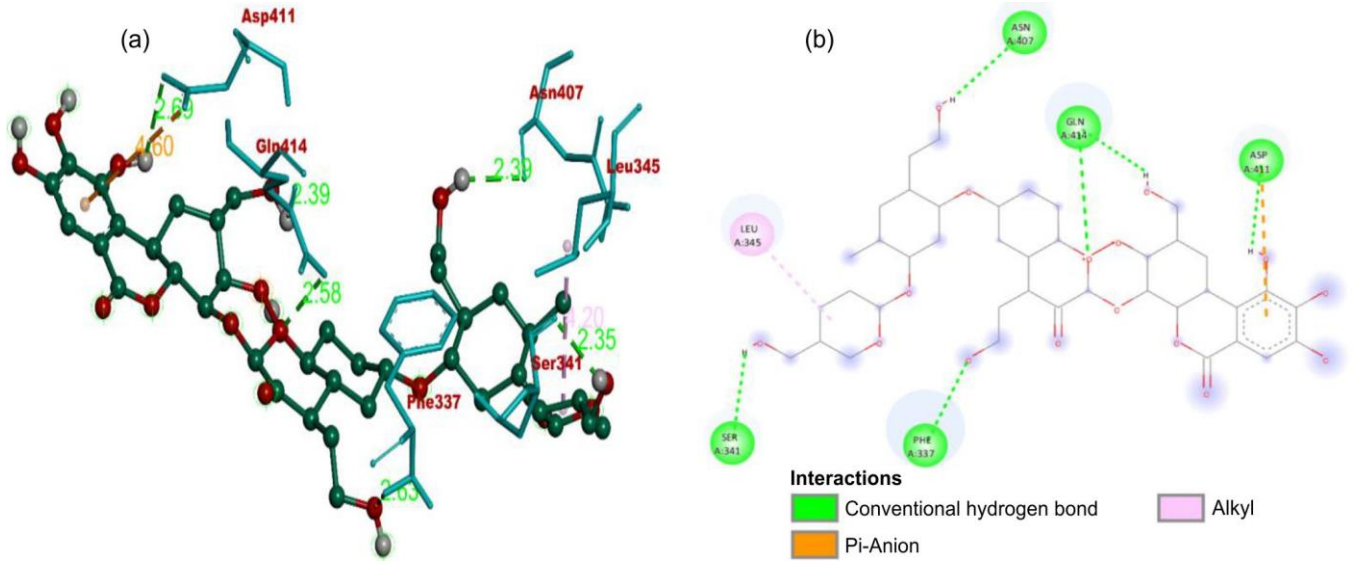

Fig. 4. Visualization of binding interactions of hypocroside (compound **1**) with the human estrogen receptor; (a) 3D representation and (b) 2D representation

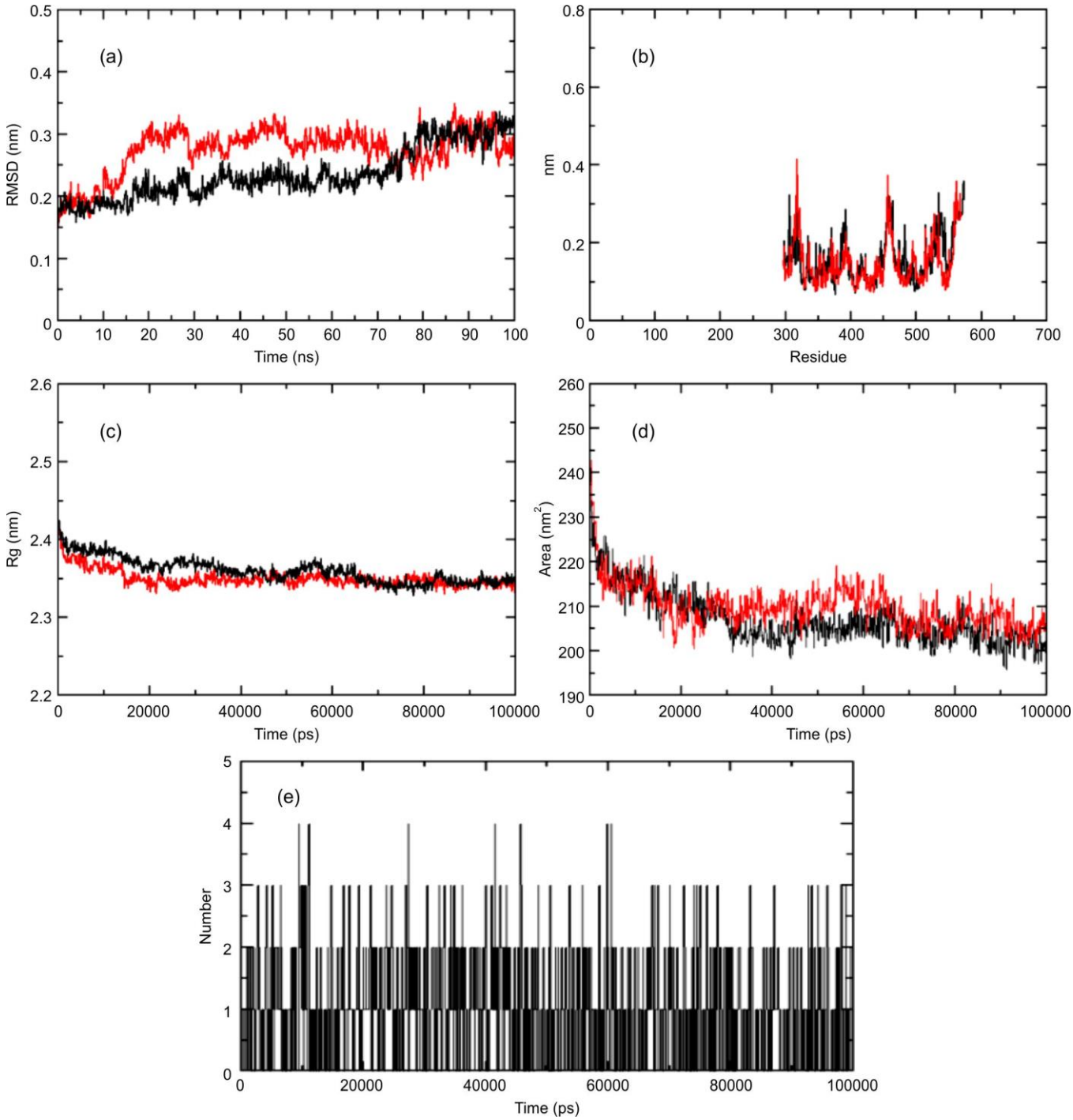

Fig. 5. Visualization of molecular dynamics trajectories of the human estrogen receptor–hypocroside (compound **1**) complex during a 100 ns simulation. (a) Protein–ligand complex RMSD, (b) Radius of gyration (Rg), (c) Root mean square fluctuation (RMSF), (d) Solvent-accessible surface area (SASA) and (e) Protein–ligand hydrogen bonds. (Red: protein backbone atoms; black: human estrogen receptor–hypocroside complex)

remaining close to 200 nm^2, indicating little variation in solvent exposure. Compound **1** maintained four hydrogen bonds with the receptor throughout the simulation, preserving stable interactions within the binding pocket. The molecular dynamics data closely matched the molecular docking results and aligned with previous reports [21]. The MD trajectories (Fig. 5) revealed that the protein-hypocroside complex remained stable over the 100 ns simulation period.

Conclusion

In this work, hypocroside (compound **1**), a novel flavonoid glycoside with antifertility activity, was isolated from *Rivea hypocrateriformis*. The compound was purified by column chromatography and its structure was elucidated using ^{1}H NMR, ^{13}C NMR, mass spectrometry, TLC and HPLC analyses. The ethyl acetate fraction (FERH) and the isolated

compound were subsequently evaluated for their anti-implantation, estrogenic and anti-estrogenic activities *in vivo* at doses of 100 and 200 mg/kg for FERH and 12.5 and 25 mg/kg for hypocroside. Both treatments exhibited anti-implantation activity, with hypocroside exhibiting higher inhibition of implantation than the ethyl acetate fraction. The reduced number of implantation sites in treated female rats establishes hypocroside as a promising candidate for antifertility therapy. Based on the results, it is suggested that hypocroside exerts its antifertility effect through modulation of estrogen-dependent reproductive pathways. Molecular docking studies also demonstrated favourable binding interactions between hypocroside and the human estrogen receptor, while molecular dynamics simulations confirmed the stability of the protein-ligand complex. These computational findings complement the biological activity observed *in vivo*.

CONFLICT OF INTEREST

The authors declare that there is no conflict of interests regarding the publication of this article.

DECLARATION OF AI-ASSISTED TECHNOLOGIES

During the preparation of this manuscript, the authors used an AI-assisted tool(s) to improve the language and no data, results or scientific conclusions were generated by AI. All analyses, interpretations and conclusions are the authors' own. The authors reviewed and edited the content and take full responsibility for the published work.

REFERENCES

1. D. Kumar, A. Kumar and O. Prakash, *J. Ethnopharmacol.*, **140**, 1 (2012); https://doi.org/10.1016/j.jep.2011.12.039
2. J.K.C. Ma, P.M.W. Drake and P. Christou, *Nat. Rev. Genet.*, **4**, 794 (2003); https://doi.org/10.1038/nrg1177
3. B. Hilal, M.M. Khan and Q. Fariduddin, *Plant Physiol. Biochem.*, **211**, 108674 (2024); https://doi.org/10.1016/j.plaphy.2024.108674
4. M. Daniyal and M. Akram, *J. Chin. Med. Assoc.*, **78**, 382 (2015); https://doi.org/10.1016/j.jcma.2015.03.008
5. H. Shivalingappa, N.D. Satyanarayan, M.G. Purohit, A. Sharanabasappa and S.B. Patil, *J. Ethnopharmacol.*, **82**, 11 (2002); https://doi.org/10.1016/S0378-8741(02)00073-9
6. S.S. Godipurge, S. Rahber, J.S. Biradar and N. Mahurkar, *Int. J. Toxicol. Pharmacol. Res.*, **7**, 65 (2015).
7. V.P. Deshmukh, in eds.: T. Pullaiah, Biomolecules and therapeutics of *Mentha rotundifolia* (L.) Huds, In: Bioactives and Pharmacology of Lamiaceae, Medicinal Plants Series, Singapore: Springer, pp. 111-127 (2023).
8. Z. Zamarrud, I. Ali, H. Hussain, V.U. Ahmad, M. Qaiser, A. Amyn and F.V. Mohammad, *Fitoterapia*, **82**, 601 (2011); https://doi.org/10.1016/j.fitote.2011.03.002
9. J. Silverman, Managing the Laboratory Animal Facility, CRC Press (2016).
10. B.A. Ferreira, R.F. Silva, F.B.R. de Moura, C.T. Narduchi, S.R. Deconte, P. Sartorelli, T.C. Tomiosso, J.H.G. Lago and F.A. Araújo, *Nat. Prod. Res.*, **36**, 5858 (2022); https://doi.org/10.1080/14786419.2021.2019729
11. W. Shibeshi, E. Makonnen, L. Zerihun and A. Debella, *Afr. Health Sci.*, **6**, 108 (2006).
12. A.M. Brzozowski, A.C. Pike, Z. Dauter, R.E. Hubbard, T.Bonn, O. Engström, L. Öhman, G.L. Greene, J.Å. Gustafsson and M. Carlquist, *Nature*, **389**, 753 (1997); https://doi.org/10.1038/39645
13. T. Maradesha, S.M. Patil, K.A. Al-Mutairi, S.V. Madhunapantula, R. Ramu and T. Alqadi, *Molecules*, **27**, 1888 (2022); https://doi.org/10.3390/molecules27061888
14. S.M. Patil, R.M. Martiz, R. Ramu, P.S. Shirahatti, A. Prakash, B.P. Kumar and N. Kumar, *J. Biomol. Struct. Dyn.*, **40**, 12491 (2022); https://doi.org/10.1080/07391102.2021.1971561
15. S.M. Patil, K.R. Maruthi, S.N. Bajpe, V.M. Vyshali, S. Sushmitha, C. Akhila and R. Ramu, *Bioinformation*, **17**, 932 (2021); https://doi.org/10.6026/97320630017932
16. N. Vasudeva and S.K. Sharma, *J. Ethnopharmacol.*, **107**, 179 (2006); https://doi.org/10.1016/j.jep.2006.03.009
17. V.C. Jordan, *Nat. Rev. Drug Discov.*, **2**, 205 (2003); https://doi.org/10.1038/nrd1031
18. A. Makker and M.M. Singh, *Med. Res. Rev.*, **26**, 699 (2006); https://doi.org/10.1002/med.20061
19. K.K. Singh, S. Parmar and P.A. Tatke, *Contraception*, **85**, 122 (2012); https://doi.org/10.1016/j.contraception.2011.04.013
20. S.A. Amin, P. Bhattacharya, S. Basak, S. Gayen, A. Nandy and A. Saha, *Comput. Biol. Chem.*, **67**, 213 (2017); https://doi.org/10.1016/j.compbiolchem.2017.01.004
21. M. Ganguly, J. Hazarika, S. Sarma, P. Bhuyan and R. Mahanta, *J. Theor. Comput. Chem.*, **19**, 2041004 (2020); https://doi.org/10.1142/S0219633620410047